Position Kinematics of a 3-$\underline{R}$RS Parallel Manipulator

Halil Tetik*, Rohit Kalla†, Gokhan Kiper*, and Sandipan Bandyopadhyay†

* Dept. of Mechanical Engineering, Izmir Institute of Technology, Izmir, Turkey

† Dept. of Engineering Design, Indian Institute of Technology Madras, India

Abstract The 3-$\underline{R}$RS parallel manipulator presented in this study comprises of parallel revolute joint axes in each leg. The manipulator is composed of a base and a moving platform which are in the shape of equilateral triangles. Moving platform has two rotational and one translational degrees-of-freedom. This study formulates the forward and inverse kinematics of the parallel manipulator. A 16th order polynomial in terms of one of the passive joint variables is obtained for the forward kinematic analysis. Numerical results and the corresponding pose of the manipulator for inverse and forward kinematics are presented.

1 Introduction

Parallel manipulators (PM) having less than 6 degrees-of-freedom (DoF) attracted a lot of attention in the past few decades due to their architectural simplicity, low cost and easier control (Fan et al. (2009)). Some of the most successful designs of PMs used in the industry are with less than 6-DoF (Chen et al. (2014)).

This study deals with a 3-DoF 3-$\underline{R}$RS PM which posseses one translational DoF and two rotary ones (Liu and Bonev (2008)). Inverse kinematic analysis of a 3-$\underline{R}$RS PM has been performed by (Li et al. (2001)), where the analysis is performed by using a geometrical approach. (Itul and Pisla (2009)) presented the inverse and forward kinematic model for a 3-$\underline{R}$RS PM. For the forward position analysis, the set of position equations are suggested to be solved numerically; no analysis as to the number of solutions is presented.

In this study, first, the geometry of the 3-$\underline{R}$RS PM is described. Then the kinematic constraints are formulated in terms of the loop-closure equations which are solved consequently. Inverse position analysis is done analytically. To solve the forward kinematic problem, the mathematical manipulation proposed by (Srivatsan and Bandyopadhyay (2013)), is applied to a set of three non-linear equations in terms of passive joint variables. Finally,

a 16th order polynomial in terms of the tangent of the half of one of the passive joint angles is obtained. The formulation is illustrated via numerical examples.

2 Position Analysis

The architecture of the PM investigated in this study is presented in Figure 1. The 3-RRS PM consists of a fixed base, a moving platform and

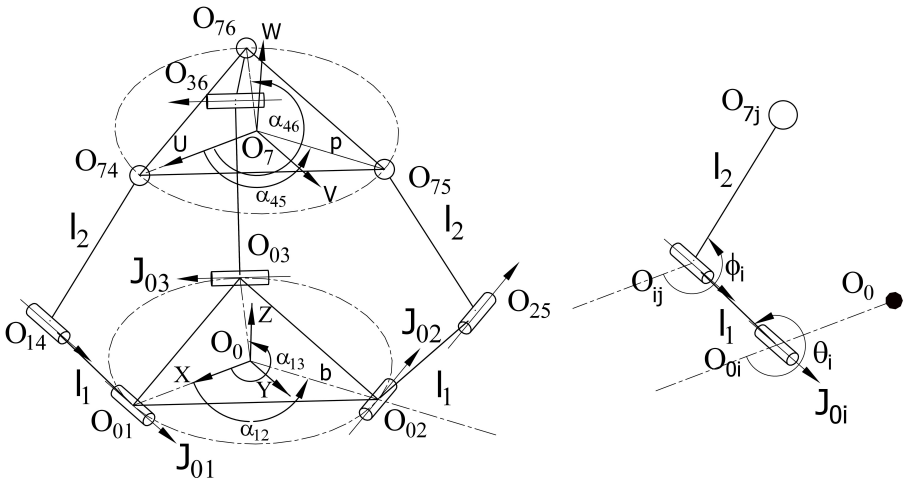

Figure 1. Kinematic model of the 3-RRS PM

three identical limbs. The ith limb is composed of three joints: active revolute (R) joint fixed on the base at the point O_{0i}; passive R joint located at the point O_{ij}; and a passive spherical (S) joint between the links having a length l_2 and the platform, located at the points O_{7j}, for $i = 1, 2, 3$ and $j = 4, 5, 6$.

In Figure 1, a fixed coordinate frame O_0-XYZ is attached to the base. Its origin, O_0, is chosen as the center of the circle with a radius of b, which is the circle tangent to all the three revolute joint axes at the base. The X-axis is along the vector $\overrightarrow{O_0O_1}$ and the Z-axis is perpendicular to the base plane. A moving coordinate frame, O_7-UVW, is attached to the platform. The origin, O_7, is attached at the center of a circle with a radius p, which is the circle passing through the three spherical joint centers. The U-axis is along $\overrightarrow{O_7O_{74}}$ vector and W-axis is perpendicular to the plane of the plat-

form. In any leg, the axes of the active and passive R joints are parallel to each other. As a specific case, to achieve a symmetric form, the points O_{0i} and O_{7j} are placed at the vertices of the base and moving platform triangles. Therefore, $\alpha_{12} = \angle O_{01}O_0O_{02} = 120°$, $\alpha_{13} = \angle O_{01}O_0O_{03} = 240°$, $\alpha_{45} = \angle O_{74}O_7O_{75} = 120°$, and $\alpha_{46} = \angle O_{74}O_7O_{76} = 240°$. The input variables are θ_1, θ_2, and θ_3; passive revolute joint variables are ϕ_1, ϕ_2, and ϕ_3.

Constraint Equations. Each limb is constrained to move in plane and the relation in between the X and Y coordinates of the spherical joint centres can be given as $O_{7j,y} = O_{7j,x}\tan(\alpha_{1i})$. Constraint equations due to this planar motion are derived by (Tsai (1999)) for a 3-R$\underline{\text{P}}$S PM and these equation are also valid for the 3-$\underline{\text{R}}$RS PM:

$$O_{7y} = -u_y p \tag{1}$$

$$O_{7x} = p(u_x - v_y)/2 \tag{2}$$

$$u_y = v_x \tag{3}$$

where O_{7x} and O_{7y} are the X and Y coordinates of the platform center, u_x, u_y, v_x, v_y are the corresponding elements of the rotation matrix and p is the radius of the circle attached to the moving platform.
O_{7z} remains independent, indicating the translational DoF along the Z-axis. To determine the elements of the rotation matrix $[\mathbf{R}]$ between coordinate frames of the base and moving platform, the following rotation sequence is applied: first rotate about the fixed Z-axis by an angle of ψ_z, then about the fixed Y-axis by an angle of ψ_y and finally about the fixed X-axis by an angle of ψ_x. This results in:

$$[\mathbf{R}] = \begin{bmatrix} u_x & v_x & w_x \\ u_y & v_y & w_y \\ u_z & v_z & w_z \end{bmatrix} = \begin{bmatrix} \mathrm{c}_y c_z & -\mathrm{c}_y \mathrm{s}_z & \mathrm{s}_y \\ s_x \mathrm{s}_y \mathrm{c}_z + c_x \mathrm{s}_z & \mathrm{c}_x c_z - s_x s_y \mathrm{s}_z & -\mathrm{s}_x \mathrm{c}_y \\ \mathrm{s}_x \mathrm{s}_z - \mathrm{c}_x \mathrm{s}_y \mathrm{c}_z & \mathrm{s}_x c_z + c_x s_y s_z & \mathrm{c}_x \mathrm{c}_y \end{bmatrix} \tag{4}$$

where s and c stand for sin and cos, respectively, and subscripts x, y and z stand for rotation angles ψ_x, ψ_y and ψ_z, respectively. $[\mathbf{R}]$ is bound to the 6 orthogonality conditions for rotation matrices. Besides, Eq. (3) further constrains $[\mathbf{R}]$. Therefore, only two elements of $[\mathbf{R}]$ are independent. Considering the workspace of the 3-$\underline{\text{R}}$RS PM, the suitable choices of independent parameters are w_x and w_y, while O_{7z}, w_x and w_y are the independent workspace parameters. For given w_x and w_y, first ψ_x, ψ_y and ψ_z can be determined:

$$\psi_y = \sin^{-1}(w_x)\,, \text{where}, s_y \neq \pm 1 \tag{5}$$

$$\psi_x = \sin^{-1}(-w_y/\mathrm{c}_y\ ) \tag{6}$$

Imposing Eq. (3) in Eq. (4), and the dividing by c_z, we can determine ψ_z as

$$\psi_z = \tan^{-1}\left(-\mathrm{s}_x\mathrm{s}_y/(\mathrm{c}_x + \mathrm{c}_y)\right) \tag{7}$$

Substituting ψ_x, ψ_y and ψ_z given by Eqs. (5)-(7), $[\mathbf{R}]$ can be determined from Eq. (4). Eqs. (1)-(2) give the dependent position parameters.

Inverse Position Analysis. Inverse kinematics problem is to find the input angles θ_1, θ_2 and θ_3 for a given pose of the moving platform. The loop-closure equation can be written as:

$$\begin{aligned}
\overrightarrow{O_0O_{7j}} &= [\mathbf{R}_Z(\alpha_{1i})]\left\{\begin{bmatrix} b \\ 0 \\ 0 \end{bmatrix} + [\mathbf{R}_Y(\theta_i)]\begin{bmatrix} l_1 \\ 0 \\ 0 \end{bmatrix} + [\mathbf{R}_Y(\phi_i)]\begin{bmatrix} l_2 \\ 0 \\ 0 \end{bmatrix}\right\} \\
\overrightarrow{O_0O_{7j}} &= \overrightarrow{O_0O_7} + [\mathbf{R}]\cdot[\mathbf{R}_Z(\alpha_{4j})]\begin{pmatrix} p \\ 0 \\ 0 \end{pmatrix}
\end{aligned} \tag{8}$$

for $i = 1, 2, 3$ and $j = i+3$. $[\mathbf{R}_Y]$ and $[\mathbf{R}_Z]$ are the elementary CCW rotation matrices about Y-, and Z-axes, respectively. We express the points O_{7j} in terms of the given pose parameters using Eq. (8). The X and Z components of Eq. (8) are:

$$l_2 c_{\phi i} c_{\alpha 1i} = O_{7jx} - c_{\alpha 1i}(b + l_1 c_{\theta i}) \tag{9}$$

$$l_2 s_{\phi i} = -O_{7jz} - l_1 s_{\theta i} \tag{10}$$

Solving $c_{\phi i}$ and $s_{\phi i}$ from the Eqs. (9)-(10), and using the identity $c_{\phi i}^2 + s_{\phi}^2 = 1$:

$$\begin{aligned}
&l_2^2(c_{\alpha 1i} + 1)^2 - [O_{7jx}c_{\alpha 1i}(b + l_1 c_{\theta i})]^2 - [c_{\alpha 1i}(O_{7jz} l_1 s_{\theta i})]^2 = 0 \\
&\Rightarrow A_i c_{\theta i} + B_i s_{\theta i} + C_i = 0
\end{aligned} \tag{11}$$

where $A_i = 2l_1 c_{\alpha 1i}(-O_{7jx} + bc_{\alpha 1i})$, $B_i = 2l_1 O_{7jz} c_{\alpha 1i}^2$ and $C_i = O_{7jx}^2 - 2bO_{7jx}c_{\alpha 1i} + c_{\alpha 1i}^2(b^2 + l_1^2 - l_2^2 + O_{7jz}^2)$. Applying tangent of half angle substitution to Eq. (11) and solving for θ_i:

$$\theta_i = 2\ \mathrm{atan2}\left(-B_i \pm \sqrt{A_i^2 + B_i^2 - C_i^2}, C_i - A_i\right) \tag{12}$$

$A_i = C_i$ results in singularity, which is not considered in this paper and it is assumed that $A_i \neq C_i$. Due to the $\pm$ sign in Eq. (12), each θ_i has two possible values, which yields at most 8 solutions. Therefore the PM has 8 assembly modes for the inverse kinematics.

Forward Position Analysis. The coordinates of the points O_{7j} can be calculated in terms of input variables θ_i and passive R joint variables ϕ_i by making use of the Eq. (8). Since the moving platform is in the form of an equilateral triangle, the distances between O_{7j} are constant and can be calculated by the cosine theorem. Using Eq. (8):

$$3p^2 = d^2 = |O_{74}O_{75}|^2 \Rightarrow f_1(\phi_1, \phi_2) = 0 \tag{13}$$

$$3p^2 = d^2 = |O_{75}O_{76}|^2 \Rightarrow f_2(\phi_2, \phi_3) = 0 \tag{14}$$

$$3p^2 = d^2 = |O_{76}O_{74}|^2 \Rightarrow f_3(\phi_1, \phi_3) = 0 \tag{15}$$

Eqs. (13)-(14) can be rewritten as:

$$f_{10} + f_{11}\mathrm{s}\phi_2 + f_{12}\mathrm{c}\phi_2 = 0 \tag{16}$$

$$f_{20} + f_{21}\mathrm{s}\phi_2 + f_{22}\mathrm{c}\phi_2 = 0 \tag{17}$$

Solving for $c\phi_2$, $s\phi_2$ from there,

$$\mathrm{s}\phi_2 = \frac{f_{12}f_{20} - f_{10}f_{22}}{f_{11}f_{22} - f_{12}f_{21}},\ \mathrm{c}\phi_2 = \frac{f_{10}f_{21} - f_{11}f_{20}}{f_{11}f_{22} - f_{12}f_{21}} \tag{18}$$

Since, $c^2\phi_2 + s^2\phi_2 = 1$, from Eq. (16)-(17), assuming $f_{11}f_{22} - f_{12}f_{21} \neq 0$:

$$(f_{12}f_{20} - f_{10}f_{22})^2 + (f_{10}f_{21} - f_{11}f_{20})^2 - (f_{11}f_{22} - f_{12}f_{21})^2 = 0 \tag{19}$$

At this point we apply the tangent of half angle substitution for the angles ϕ_1 and ϕ_3 for Eqs. (13)-(15): $t_1 = \tan(\phi_1/2)$ and $t_3 = \tan(\phi_3/2)$. Eq. (17) involves t_1 and t_3, only. Rearranging Eq. (17), it is seen that it is a 4th degree polynomial in t_1:

$$a_0 + a_1t_1 + a_2t_1^2 + a_3t_1^3 + a_4t_1^4 = 0 \tag{20}$$

Coefficients a_i in Eq. (20) are also 4th degree polynomials in t_3. Also rearranging Eq. (15) in terms of t_1 results in a quadratic equation:

$$b_0 + b_1t_1 + b_2t_1^2 = 0 \tag{21}$$

The coefficients b_i are also 2nd degree polynomials in terms of t_3. Eliminating t_1 from Eqs. (20)-(21) using polynomial division, we obtain:

$$\frac{b_2^3 H}{\left[a_4b_1^3 - b_1\left(2a_4b_0 + a_3b_1\right)b_2 + \left(a_3b_0 + a_2b_1\right)b_2^2 - a_1b_2^3\right]^2} = 0 \Rightarrow H = 0 \tag{22}$$

where

$$
\begin{aligned}
H =& a_4 \left\{ a_4 b_0^4 + b_1 \left[-a_3 b_0^3 + b_1 \left(a_2 b_0^2 - a_1 b_0 b_1 + a_0 b_1^2 \right) \right] \right\} + b_2 \left(a_3^2 - 2a_2 a_4 \right) b_0^3 + \\
& b_2^2 \left[\left(a_2^2 - 2a_1 a_3 + 2a_0 a_4 \right) b_0^2 + \left(-a_1 a_2 + 3a_0 a_3 \right) b_0 b_1 + a_0 a_2 b_1^2 \right] + \\
& \left(-a_2 a_3 + 3a_1 a_4 \right) b_0^2 b_1 + \left(a_1 a_3 - 4a_0 a_4 \right) b_0 b_1^2 - a_0 a_3 b_1^3 + \\
& b_2^3 \left[\left(a_1^2 - 2a_0 a_2 \right) b_0 - a_0 a_1 b_1 \right] + a_0^2 b_2^4
\end{aligned}
$$

Eq. (22) is valid provided that $b_2 \neq 0$ and also denominator in Eq. (22) is nonzero. Eq. (22) is a 16th order polynomial in terms of t_3. The value of t_3 can be numerically computed from Eq. (22). For any t_3 value, t_1 is determined from Eqs. (20)-(21) and ϕ_2 is given by Eq. (16). There are at most 16 assembly modes of the moving platform for the forward kinematics. Once the platform points O_{7j} are determined from Eq. (8), the location of the platform is determined.

3 Numerical Example

Several numerical examples are worked out in order to check forward and inverse kinematic solutions using `Mathematica`. As an example, consider the case where $b = 0.55$ m, $p = 0.275$ m, $l_1 = 0.7$ m and $l_2 = 0.775$ m. For the inverse kinematic analysis, as a generic example for given pose parameters $O_{7z} = 1.2$ m, $w_x = -0.2$ and $w_y = 0.2$, the possible corresponding joint angles are found as $(\theta_1, \theta_2, \theta_3)$=$(-71.60°, -66.09°, -68.57°)$, $(-133.61°, -144.85°, -136.47°)$. Any of two solutions for an angle is valid and there are totally eight solutions.
To verify the forward kinematic formulation, let $\theta_1 = -133.61°$, $\theta_2 = -144.85°$ and $\theta_3 = -136.47°$, which is one of the eight solutions above. The solution of the 16th order univariate polynomial in terms of t_3 results in sixteen distinct real solutions. The numerical values obtained for t_3, corresponding passive joint variables ϕ_i and task space variables O_{7z}, w_x and w_y are presented in Figure 2. Notice that the 6th set of solutions matches with the task space parameters used in the inverse kinematic analysis. Figure 2 depicts the poses of the PM for the corresponding solutions.

4 Conclusion

A detailed analysis for the forward and inverse kinematics analysis of the 3-$\underline{\text{R}}$RS PM is presented in this study. For the forward kinematics, all but one dependent joint variables are eliminated to obtain a 16th order polynomial. This suggests that an upper bound for the forward kinematics solutions of the 3-$\underline{\text{R}}$RS PM is 16, which proves that polynomial obtained is the smallest

1	2	3
t_3=-2.07 ϕ_1=-56.04° ϕ_2=-92.32° ϕ_3=-128.40° w_x=-0.034 w_y=-0.18 $O_{7,z}$=1.14 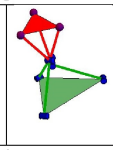	t_3=-1.73 ϕ_1=-52.21° ϕ_2=-103.26° ϕ_3=-119.88° w_x=-0.09 w_y=0.01 $O_{7,z}$=1.14 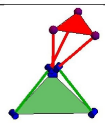	t_3=-1.55 ϕ_1=-116.11° ϕ_2=-108.70° ϕ_3=-114.26° w_x=0.10 w_y=-0.11 $O_{7,z}$=1.18 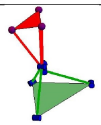
4	5	6
t_3=-1.50 ϕ_1=-117.81° ϕ_2=-48.51° ϕ_3=-112.58° w_x=0.25 w_y=-0.45 $O_{7,z}$=1.12 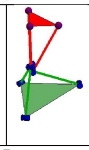	t_3=-0.85 ϕ_1=-66.85° ϕ_2=-126.22° ϕ_3=-80.99° w_x=-0.20 w_y=0.46 $O_{7,z}$=1.16 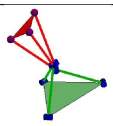	t_3=-0.73 ϕ_1=-74.88° ϕ_2=-68.66° ϕ_3=-72.22° w_x=-0.2 w_y=0.2 $O_{7,z}$=1.2 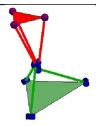
7	8	9
t_3=-0.56 ϕ_1=-135.65° ϕ_2=-83.84° ϕ_3=-58.95° w_x=0.27 w_y=-0.06 $O_{7,z}$=1.12 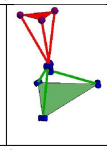	t_3=-0.47 ϕ_1=-123.46° ϕ_2=-101.73° ϕ_3=-50.74° w_x=0.08 w_y=0.17 $O_{7,z}$=1.13 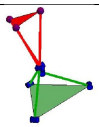	t_3=0.53 ϕ_1=97.19° ϕ_2=124.38° ϕ_3=55.72° w_x=-0.16 w_y=-0.16 $O_{7,z}$=-0.22
10	11	12
t_3=0.70 ϕ_1=77.16° ϕ_2=132.07° ϕ_3=69.88° w_x=0.10 w_y=-0.15 $O_{7,z}$=-0.22 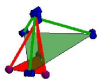	t_3=0.73 ϕ_1=74.56° ϕ_2=67.86° ϕ_3=72.45° w_x=-0.11 w_y=0.12 $O_{7,z}$=-0.27	t_3=0.89 ϕ_1=133.47° ϕ_2=57.43° ϕ_3=83.36° w_x=-0.51 w_y=-0.08 $O_{7,z}$=-0.20

13	14	15	16
t_3=1.17 ϕ_1=57.04° ϕ_2=121.93° ϕ_3=98.87° w_x=0.30 w_y=0.06 $O_{7,z}$=-0.23	t_3=1.56 ϕ_1=115.73° ϕ_2=107.43° ϕ_3=114.55° w_x=0.21 w_y=-0.24 $O_{7,z}$=-0.25	t_3=1.65 ϕ_1=112.62° ϕ_2=43.42° ϕ_3=117.63° w_x=-0.10 w_y=0.16 $O_{7,z}$=-0.18	t_3=2.27 ϕ_1=87.89° ϕ_2=55.20° ϕ_3=132.54° w_x=0.26 w_y=0.30 $O_{7,z}$=-0.20

Figure 2. Forward kinematic solutions

one. The formulations are implemented in `Mathematica` and several numerical examples are presented. Indeed 16 real solutions are obtained for some configurations.

The formulations developed here will be implemented for the control of a 3-RRS PM in Izmir Institute of Technology. Further studies would include the identification of singularities and safe working zone, (see, Srivatsan and Bandyopadhyay (2014)) and dynamic analyses of the PM.

Bibliography

Xiang Chen, FG Xie, XJ Liu, F Xie, and T Sun. A comparison study on motion/force transmissibility of two typical 3-DoF parallel manipulators: the sprint Z3 and A3 tool heads. *International Journal of Advanced Robotic System*, 11(5):1–10, 2014.

Caixia Fan, Hongzhao Liu, and Yarbin Zhang. Kinematics and singularity analysis of a novel 1T2R fully-decoupled parallel mechanism. In *Intelligent Computing and Intelligent Systems, 2009. ICIS 2009. IEEE International Conference*, volume 2, pages 312–316. IEEE, 2009.

Tiberiu Itul and Doina Pisla. Kinematics and dynamics of 3-DoF parallel robots with triangle platform. *Journal of Vibroengineering*, 11(1), 2009.

Jianfeng Li, Jinsong Wang, Wusheng Chou, Yuru Zhang, Tianmiao Wang, and Qixian Zhang. Inverse kinematics and dynamics of the 3-RRS parallel platform. In *Robotics and Automation, 2001. Proceedings 2001 ICRA. IEEE International Conference*, volume 3, pages 2506–2511. IEEE, 2001.

Xin-Jun Liu and Ilian A Bonev. Orientation capability, error analysis, and dimensional optimization of two articulated tool heads with parallel kinematics. *Journal of Manufacturing Science and Engineering*, 130(1): 011015–011015–9, 2008.

R Arun Srivatsan and Sandipan Bandyopadhyay. On the position kinematic analysis of MaPaMan: A reconfigurable three-degrees-of-freedom spatial parallel manipulator. *Mechanism and Machine Theory*, 62:150–165, 2013.

R Arun Srivatsan and Sandipan Bandyopadhyay. Determination of the Safe Working Zone of a Parallel Manipulator. In *Computational Kinematics*, pages 201–208. Springer, 2014.

Lung-Wen Tsai. *Robot analysis: The Mechanics of Serial and Parallel Manipulators*. John Wiley & Sons, 1999.